DFT Cluster Calculations for Alkali Cation-Exchanged Zeolites Interacting with Ethylchloride and HCl

Rodrigo J. Corrêa,[†] E. Falabella Sousa-Aguiar,[‡] A. Ramirez-Solís,[§] Claudio Zicovich-Wilson,[§] and Claudio J. A. Mota*[,†]

Instituto de Química, Universidade Federal do Rio de Janeiro Cidade Universitária CT Bloco A, 21949-900 Rio de Janeiro, Brazil, PETROBRAS/CENPES, Cidade Universitária, Ilha do Fundão, Rio de Janeiro, 21949-900 Brazil, and Dpto de Física, Facultad de Ciencias, Universidad Autónoma del Estado de Morelos, Av. Universidad 1001, Col. Chamilpa, Cuernavaca, Morelos 62210, Mexico

Received: November 4, 2003; In Final Form: April 27, 2004

T_5 and T_8 clusters (T = Si, Al) were used to calculate the structure of alkali cation-exchanged zeolites using DFT-based methods. The activity of basic zeolites was estimated from reactions with HCl and ethylchloride proton elimination. For the first case, all of the zeolite clusters reacted exothermically, with LiT_5 presenting a $\Delta H = -29.7$ kcal/mol and CsT_5 showing a $\Delta H = -24.7$ kcal/mol at the B3LYP/6-311+G** level of theory. For the proton elimination from ethylchloride to form ethene, only the LiT_5 cluster had an exothermic reaction. The other clusters had a ΔH varying from +0.1 kcal/mol for NaT_5 to +2.3 kcal/mol for CsT_5. The activation barriers for this reaction increased from Li to Cs. A careful analysis of the geometries, charges, and energetics for adsorption and activation barriers has shown that the reaction is controlled by the Lewis acid/base interaction between the cation and the chloride ion, not involving the Bronsted basicity of the framework oxygen atoms. These reactions proceed through a concerted mechanism that simultaneously involves the zeolitic basic framework oxygen atoms and the cation, which acts as a Lewis acid.

I. Introduction

Zeolites are aluminosilicates with a 3D structure forming channels and cages with molecular dimensions. The aluminum atoms in the zeolite framework are tetracoordinated, which requires a compensating extraframework cation to neutralize the whole structure. Ion exchange techniques are normally employed to change the cations inside the cages, thereby changing the acid−base character. Zeolite acid catalysis is much more important than basic catalysis because of the fact that acidic zeolites are important catalysts in petroleum refining. However, as the use of zeolites in fine chemicals grows, basic catalysis will become important too, with possible applications in aldol condensation.

Exchanging alkali metals, such as Cs^+ and Rb^+ in X or Y zeolites normally produces basic catalysts.[1] A simplistic view of zeolite basicity takes into account that the more electropositive the compensating cation is the larger the negative charge developed on the structure, particularly on the framework oxygen atoms.[2]

The basicity can also be analyzed using the hardness/softness concept[3] because for species with a given fixed charge, the hardest can be characterized as the one having the largest charge/volume ratio; therefore, for alkaline cations, the hardness will follow the Cs^+-to-Li^+ sequence in the periodic table.

Zeolite acidity has been characterized by many techniques. However, the measurement of zeolite basicity is still a matter of intense research. Pyrrole has been used as a probe molecule to measure the basicity of X and Y zeolites. By measuring the frequency of the infrared stretching N−H mode, one can compare the basicity of different zeolites.[4] For instance, upon adsorption on LiX, the stretching NH band of pyrrole is observed at 3295 cm^{-1}, whereas on CsX, this band appeared at 3175 cm^{-1}. The lower wavenumber on CsX indicated that the NH band was weaker compared to that of LiX.[5] Pyrrole adsorption on X zeolites has also been studied[6] by XPS. It was found that the binding energy for the N(1s) electrons is influenced by the nature of the compensating cation. It decreases from Li to Cs on X and Y zeolites. Other molecules such as benzene,[7] carbon dioxide,[8] acetic acid,[9] and HCN[10] have also been used to characterize zeolite basicity. Solid-state NMR of chloroform adsorbed on alkaline-exchanged zeolites indicated[11] that the C−H bond becomes more polarizable going from LiY to CsY. Another feature found is that an X zeolite is polarized more than a Y zeolite. The result is explained in terms of an interaction between the framework oxygen atoms and the acidic proton. UV−vis diffuse reflectance spectroscopy of adsorbed iodine proved[12] that there is a linear correlation between the partial charge on the zeolite oxygen atoms and the I_2 molecule. Such an observation confirms that iodine interacts with the basic oxygen atoms instead of the charge-balancing cations. The photoreduction of methyl viologen (MV^{2+}) was studied[13] in a series of alkali-exchanged X zeolites. The photoyielded cation radical ($MV^{+\cdot}$) and the donor strength of the zeolite framework increase in the order of $Li-X/MV^{2+} < Na-X/MV^{2+} < K-X/MV^{2+} < Rb-X/MV^{2+} < Cs-X/MV^{2+}$. This is supported by a linear correlation of the photoyields of the probe cation radical inside zeolite X with Sanderson's partial charges on the framework oxygen atoms.

Sánchez-Sánchez et al. have measured[14] the ^1H and ^{13}C NMR longitudinal relaxation times (T1) of $CHCl_3$ and $^{13}CHCl_3$ adsorbed over alkali-exchanged faujasites. Their results suggest

* Corresponding author. E-mail: cmota@iq.ufrj.br.
[†] Universidade Federal do Rio de Janeiro.
[‡] Cidade Universitária.
[§] Universidad Autónoma del Estado de Morelos.

10.1021/jp037353f CCC: $27.50
Published on Web 06/22/2004

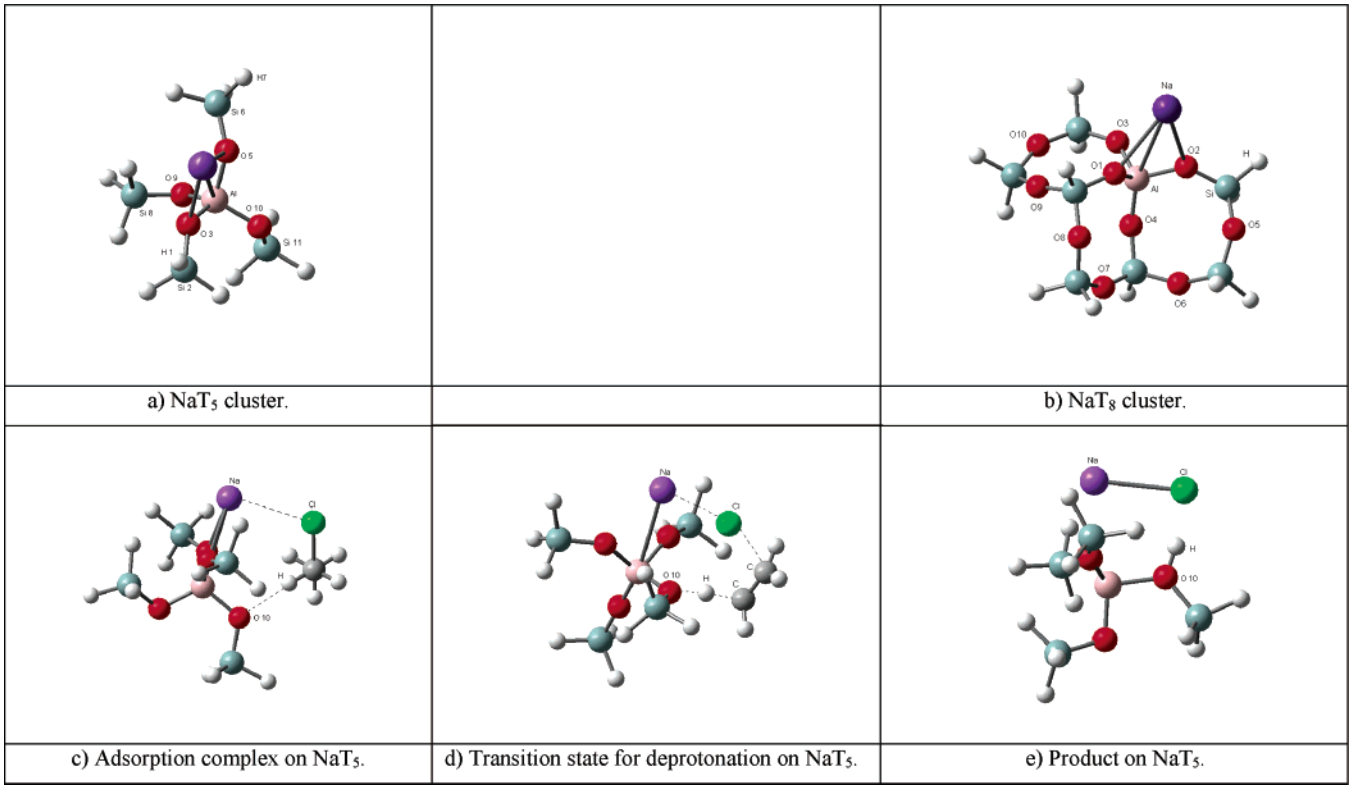

Figure 1. MT_5 and MT_8 structures.

that the mobility of the adsorbed molecules at room temperature depends on the zeolite basicity obtained by Sanderson's methodology. A study of ammonia sorption[15] on alkali metal-exchanged X zeolites found that the equilibrium sorption uptake at 50 Torr and above 100 °C follows the order NaX > NaKX > NaRbX > NaCsX. Moreover, the *c* value (related to the heat of sorption during monolayer formation) obtained from the isotherm equation reveals that the charge densities of the cations influence the interaction between NH_3 and zeolites from NaX > NaKX > NaRbX > NaCsX.

Theoretical methods are also employed to investigate the concept of basic centers in solid materials using ab initio methods or the electronegativity equalization method developed by Sanderson (EEM). Vayssilov et al. calculated[16] the O (1s) binding energies in cyclic clusters containing five and six T atoms using a DFT-derived method. They also related charge to the basicity concept. Heidler and co-workers used[17] modified EEM and Monte Carlo techniques to study the basicity of faujasite-type zeolites. Results show that the main factor influencing the zeolite basicity is the framework composition. The negative charge on the oxygen atom increases as the Si/Al ratio decreases and by exchanging Na^+ and Cs^+ atoms. Deka et al. calculated[18] the local softness and relative nucleophilicity values from DFT methods on a T_3 cluster and concluded that the larger the cation, the more basic the oxygen atoms in the cluster. Although several efforts have been directed at locating and calculating the magnitude of the negative charges on the zeolite structure, whether the charge is the main feature responsible for the basicity is still a matter of controversy.

In recent work, some of us reported[19] that butyl chlorides adsorb onto the NaY zeolite, giving rise to S_N2-type reactions, with the formation of the respective alkoxide, or E_2-type proton elimination. The extent of each reaction depends on the butylchloride structure. For primary and secondary chlorides, alkoxide formation is preferred, whereas proton elimination to give isobutene is preferential with *tert*-butylchloride. Calculations confirmed the experimental results, showing that alkoxide formation has a lower energy barrier for primary and secondary chlorides compared with that for proton elimination.

Because the role played by the alkali cation has been shown to be crucial, in this work, we study the reaction profiles between a simpler halogenated hydrocarbon (ethylchloride) with a $M-T_5$ cluster, where M goes from Li to Cs. For a more detailed study of basicity, we have also considered the case of HCl interacting with the same clusters. In both cases, the cluster acts as a base, abstracting a proton from the ethylchloride to form ethene or from HCl to form an acidic T_5 cluster and a metal chloride moiety.

II. Computational Details

The framework of the MT_5 cluster was taken from the published data[20] of the faujasite structure. To keep the original zeolite structure and to reduce computational time during geometry optimizations, we fixed four dihedral angles: {H1Si2O3Al (144.6°), Si2O3AlO5 (142.6°), H7Si6O5Al (168.5°), and O3AlO5Si6 (121.1°)} as well as two bond angles {Si8O9Al (109.3°) and Si11O1Al (121.1°)}. The atom numbering appears in Figure 1a. Calculations of reactant species and products were performed at the B3LYP/6-311+G**//B3LYP/6-31+G** level of theory. For K, Rb, and Cs cations, a relativistic effective core potential[21] (RECP) was used.

For a deeper study of the charges on the metal and framework oxygen atoms, we have also constructed a larger MT_8 cluster. This cluster was extracted from the same faujasite structure, but in this case, all three four-membered rings are properly represented; the geometry optimization was done without restrictions, and the cluster was saturated with hydrogen atoms (Figure 1b). The geometries were optimized at the B3LYP/6-31+G**//B3LYP/6-31G* level of theory. It must be pointed out that this larger cluster was not used to study the reaction mechanisms. The geometry of the metal−zeolite clusters (MT_5)

TABLE 1: Main Geometric Parameters for Reactants for MT_5 and MT_8, Adsorption Complexes, Transition Structures, and Products on MT_5[a,b]

structure	metal	M−Al	M−Cl	O10H	H−Cl	CH#	CCl	O−Al−O*
reactant T_5	Li	2.547						93.3
	Na	2.925						99.6
	K	3.368						100.9
	Rb	3.613						102.7
	Cs	3.842						104.1
reactant T_8	Li	2.557						91.3
	Na	2.932						95.5
	K	3.390						101.3
	Rb	3.500						101.9
	Cs	3.592						102.6
adsorption T_5	Li	2.559	2.407	2.360			1.868	93.8
	Na	2.935	2.610	2.280			1.861	99.4
	K	3.390	3.270	2.370			1.858	101.9
	Rb	3.630	3.450	2.240			1.857	103.5
	Cs	3.870	3.680	2.250			1.850	104.7
transition stateT_5	Li	2.593	2.190	1.300		1.343	2.628	95.5
	Na	2.912	2.531	1.268		1.366	2.588	100.2
	K	3.270	2.940	1.270		1.348	2.555	104.3
	Rb	3.486	3.136	1.262		1.366	2.554	105.8
	Cs	3.750	3.399	1.250		1.361	2.542	107.0
productT_5	Li	2.564	2.229	1.033	1.901			98.6
	Na	2.930	2.550	1.043	1.852			103.3
	K	3.390	2.922	1.050	1.820			105.7
	Rb	3.668	3.180	1.060	1.790			107.4
	Cs	3.952	3.180	1.060	1.770			108.0

[a] Distances measured in angstroms; angles measured in degrees. [b] See Figure 1 for oxygen numbering on MT_5 and MT_8.

and ethylchloride were initially separately optimized. From these optimized geometries, we obtained the structures corresponding to the adsorption minima of the ethylchloride products and the zeolite clusters. The latter structures were then used in the search for the transition states (TS) using the Berny and eigenvalue following (EF) algorithms. It should be stressed that no constraint was imposed on the system when calculating the transition states, which were characterized as having only one imaginary frequency, which corresponds to the reaction mode.

The products were assumed to be free ethene and the protonated $MClT_5$ (Figure 1c). A vibrational analysis was performed for all structures, and the frequencies were scaled by 0.96 to obtain the zero-point energy (ZPE) and thermal corrections to 298.15 K. Unless otherwise stated, all energy differences refer to enthalpy. In both clusters, charges at the atomic centers were calculated by fitting the density-derived electrostatic potential with the CHelpG scheme[22] using the B3LYP/6-311+G** wave functions. All calculations were performed using the Gaussian 98 package.[23]

III. Results and Discussion

A. Geometries and Charge Calculations for MT_5 and MT_8. Figure 1a and b shows the optimized geometries for the NaT_5 and NaT_8 clusters. Table 1 shows some selected geometrical parameters for the MT_5 and MT_8 structures. In all of the MT_5 structures, the alkali cation is located above the framework Al atom, lying almost in the O3AlO5 plane, as seen in Figure 1a. The M−Al distance varies from 2.547 Å for Li^+ to 3.842 Å for Cs^+ in the MT_5 cluster. As a general trend, the geometric parameters for the MT_8 clusters show the same behavior as that found on MT_5 (Table 1). Both the M−Al distances and the O1AlO2 angle increase from Li^+ to Cs^+ as the metal radii grow. Comparing the variations in M−Al length, one can see a pronounced contraction for Rb^+ and Cs^+ on going from T_5 to T_8 clusters. This is due to the fact that these alkali atoms move away from the O1AlO2 plane toward the O3 atom, thus getting closer to the central Al atom.

Tables 2 and 3 present the density-derived electrostatic potential charges on the oxygen atoms near the framework aluminum and the metal for the MT_5 and MT_8 models, respectively. In both cases, the general trend is to decrease the charge separation between the Al and neighboring oxygen atoms (with a slight inversion in the case of K^+ and Rb^+ for MT_8) as the atomic number of the alkali cation increases, as can be seen from the average charges on the oxygen atoms, ⟨O⟩, and the Al atom. Thus, Li^+ is the one that produces the largest average polarization of the Al−O bonds. This might be explained in two possible ways: (a) the Lewis acid character of Li^+ induces an electron transfer from the oxygen atoms toward the cation, and thus, according to Gutmann's rule,[24] the Al−O bonds become more ionic because the Al−O distances increase or (b) the cation (Li^+) induces a larger polarization of the bridging oxygen lone pairs, thus leading to a change from sp^3 to sp^2 hybridization with the concomitant change in Al−O bond ionicity. Of course, as the ionic radius of the alkali cation grows, this effect becomes less important, in agreement with the present results. It is generally believed that the oxygen atoms of the structure play the role of a Brönsted basic center. Thus, the larger the negative charge is on the atom, the more basic character the zeolite will have. Using the Sanderson electronegativity principle, many authors conclude that a more electropositive cation, such as Cs^+, will develop a more intense charge on the framework. Our results point in a completely different direction, as can be seen in Tables 2 and 3, indicating that zeolite basicity

TABLE 2: ChelPG Charges and Charge Variations on T_5 Clusters

	metal	O3	O5	O9	O10	⟨O⟩	Al	metal	H	Cl
reactants	Li	−0.870	−0.886	−0.809	−0.725	−0.823	1.425	0.806		
	Na	−0.834	−0.857	−0.752	−0.739	−0.796	1.399	0.844		
	K	−0.732	−0.799	−0.798	−0.725	−0.764	1.395	0.791		
	Rb	−0.716	−0.782	−0.803	−0.723	−0.756	1.393	0.799		
	Cs	−0.684	−0.780	−0.783	−0.717	−0.741	1.369	0.793		
adsorption complex	Li	−0.796	−0.811	−0.724	−0.657	−0.741	1.334	0.754	−0.054	−0.282
	Na	−0.794	−0.816	−0.722	−0.641	−0.743	1.319	0.821	−0.048	−0.311
	K	−0.707	−0.719	−0.709	−0.656	−0.698	1.258	0.783	−0.028	−0.309
	Rb	−0.688	−0.701	−0.706	−0.661	−0.690	1.246	0.787	−0.020	−0.305
	Cs	−0.668	−0.680	−0.712	−0.664	−0.681	1.230	0.777	−0.018	−0.305
transition state	Li	−0.748	−0.740	−0.503	−0.577	−0.642	1.111	0.776	0.272	−0.648
	Na	−0.708	−0.743	−0.509	−0.715	−0.669	1.109	0.776	0.443	−0.686
	K	−0.583	−0.654	−0.587	−0.676	−0.625	1.010	0.725	0.440	−0.652
	Rb	−0.589	−0.656	−0.622	−0.698	−0.641	1.034	0.719	0.464	−0.643
	Cs	−0.564	−0.634	−0.572	−0.623	−0.598	1.012	0.718	0.473	−0.642

TABLE 3: ChelpG Charges on T_8 Clusters

metal	O1	O2	O3	O4	⟨O⟩	M	Al	O5	O6	O7	O8	O9	O10	⟨O⟩
Li	−1.045	−0.894	−1.001	−0.885	−0.956	0.864	1.655	−0.725	−0.650	−0.661	−0.690	−0.682	−0.694	−0.684
Na	−0.970	−0.862	−0.924	−0.913	−0.917	0.866	1.609	−0.738	−0.629	−0.658	−0.768	−0.708	−0.725	−0.704
K	−0.868	−0.877	−0.872	−0.886	−0.876	0.814	1.568	−0.710	−0.622	−0.666	−0.726	−0.651	−0.712	−0.681
Rb	−0.919	−0.870	−0.863	−0.866	−0.880	0.834	1.585	−0.730	−0.654	−0.658	−0.669	−0.698	−0.718	−0.688
Cs	−0.800	−0.878	−0.876	−0.879	−0.858	0.816	1.563	−0.701	−0.647	−0.671	−0.654	−0.668	−0.716	−0.676

TABLE 4: Energetic Profiles for the Reactions between MT_5 and Ethylchloride

MT_5	$\Delta H_{adsorption}$ (kcal/mol)	$\Delta H^{\ddagger}_{activation}$ (kcal/mol)	$\Delta H_{reaction}$ (kcal/mol)
LiT_5	−15.2	24.7	−2.7
NaT_5	−9.8	25.2	0.1
KT_5	−9.3	26.8	1.8
RbT_5	−9.1	26.4	1.4
CsT_5	−8.7	28.2	2.3

is more complex than just considering electronegativity concepts. The same trend was found when we calculated the charge distribution in isolated alkaline metal hydroxide structures. In LiOH, the charge on the cation is the highest (+0.918) among the series, whereas in CsOH, the charge on the cation is the lowest (+0.829) among the calculated alkaline metal hydroxides. These results stress the previous discussion on MT_5 clusters.

B. Reaction of MT_5 with Ethylchloride. This reaction proceeds through a concerted mechanism where the chlorine atom interacts with the cation in the cluster and, simultaneously, a proton from ethylchloride is transferred to the O10 atom in the cluster. Thus, these results strongly suggest that the MT_5 clusters act as Lewis acid/base pairs. Table 4 shows the energetic profiles for these reactions on MT_5 clusters. One can clearly see a trend in the thermodynamics and the kinetic behavior along the alkali series. LiT_5 was the only zeolite cluster that gave a slightly exothermic reaction for proton elimination from ethylchloride. All other reactions had weakly endothermic behavior, with ΔH increasing from Na^+ to Cs^+. The same trend was observed for the activation energy. LiT_5 showed the lowest activation energy (24.7 kcal/mol), whereas CsT_5 showed the highest (28.2 kcal/mol). Although we are perfectly aware that some energy differences are within the error bars associated with this level of calculation, we can stress that a trend is clearly apparent. Again, K^+ and Rb^+ show practically the same behavior for this reaction.

The adsorption complexes for the interaction of MT_5 and ethylchloride show a strong interaction between the cation and the chlorine atom. The metal cation is pulled out from the cluster, as can be observed in Figure 1c. This kind of behavior was observed in previous calculations[19] of NaT_3 interactions with butyl chlorides. Table 1 highlights such behavior: (1) The M−Cl distance grows from Li^+ to Cs^+, which seems to be directly related to the ionic radius of the cation. (2) Regardless of the cation, the $O_{10}H^*$ bond (hydrogen interaction between O_{10} and the H* on C_1) varies only slightly. This may suggest that the Lewis acid/base interaction prevails over the Brönsted basicity in the elimination reaction, where the alkaline metal cations act as Lewis acids. This also agrees with the fact that a slight variation in the charges is observed for the isolated cluster. (3) The C−Cl distance increases from CsT_5 to LiT_5, showing that, as the size of the cation grows, (smaller charge/radius ratio), there is less covalent character in this metal−chlorine interaction.

The transition states (TS) show that the chlorine atom is being partially released from the ethylchloride molecule, whereas the $CH^{\#}$ (the bond in the C2 carbon of ethylchloride) is being broken in a concerted way. The $CH^{\#}$ bond in pure ethylchloride is 1.130 Å at the same level of calculation. In the TS, this bond increases approximately 0.2 Å, showing a small variation of 0.05 Å from Li to CsT_5.

The structure of the products shows the formation of a M−Cl bond and the H−O bond in T_5; it can also be seen that ethylene is desorbed. The M−Cl bond increases continuously in the series Li^+ to Cs^+, as a consequence of the cation radius. There is a hydrogen bond between the chloride ion and the proton attached to the cluster (HT_5). This bond is stronger for the cesium chloride, and weaker for lithium chloride, as measured by the H- - -Cl distance; this can arise from the more ionic nature of the isolated cesium chloride moiety.

The average charge on the oxygen atoms of the MT_5 cluster shows a small decrease when going from the free cluster to the adsorption complex. The same thing happens when going from the adsorption complex to the TS. This can be explained by the fact that, as the cation−chlorine interaction becomes stronger the inductive effect of the former on the Al−O bonds in the cluster decreases as a result of the back-donation from the chloride ion to the cation. This also explains why this effect is more pronounced for the LiT_5 cluster. The general trend in the adsorption and the TS for proton elimination from ethylchloride on MT_5 clusters is consistent with the previous report[20] of the same reaction in butylchlorides on NaT_3.

TABLE 5: Enthalpies for the Reactions between MT_5 and HCl

MT_5	$\Delta H_{reaction}$ (kcal/mol)
LiT_5	−29.7
NaT_5	−26.8
KT_5	−25.2
RbT_5	−25.5
CsT_5	−24.7

These trends can be explained by the fact that this reaction is mainly driven by the cation−chlorine interaction. Accordingly, Li^+ is the strongest and the hardest Lewis acid of the series, and both properties decrease as the radii of the cations increase. Therefore, the acid−base interaction with the chlorine atom weakens along the Li^+ to Cs^+ series, leading to larger M−Cl bond lengths (Table 1) together with less stable products and reaction intermediates (transition states). Additionally, the fact that the chloride ion is a hard base explains the largest affinity with the Li^+ cation.

C. Reaction of MT_5 with HCl and Correlation with the HSAB Principle. Table 5 shows the energy involved in the reaction between MT_5 clusters and HCl. This is a typical Brönsted acid/base reaction; therefore, it can provide significant information regarding the basicity of the zeolites. All of the alkali metal-exchanged clusters reacted exothermically but once again, LiT_5 had the most exothermic reaction within the series (−29.7 kcal/mol), whereas the reaction with CsT_5 is the less exothermic (−24.7 kcal/mol). This result is in contradiction to the accepted view that Cs-exchanged zeolites are usually employed as basic catalysts, rather than Li-exchanged zeolites. Actually, the cation plays the role of the conjugated acid to the basic species (in this case the zeolite active site), thus the stronger the Lewis acidity of the cation, the weaker the basicity of the conjugated base. In the present case, with the reactions of chlorinated compounds, what drives the reaction, as previously discussed, is not really the Bronsted basicity associated with the framework oxygen atoms but the Lewis acidity of the cation. This can be linked to Pearson's hardness and softness concepts; the hardest acid (Li^+) will be the best reactant with a hard base such as Cl^-. It might be possible that with softer acids, such as ketones, the basic character of the framework oxygen atoms prevails over the Lewis acidity associated with the metal cations. The same explanation was recently used to explain the interaction of pyrrole with alkaline cation-exchanged zeolites.[25]

IV. Conclusions

Calculations at the B3LYP/6-311+G**//B3LYP/6-31+G** level have been performed for the proton elimination from ethylchloride on MT_5 clusters (M = Li, Na, K, Rb, and Cs). This reaction is only exothermic for the LiT_5 cluster and is endothermic for the other alkaline cation T_5 clusters. A careful analysis of the geometries, charges, and energetics for adsorption and activation barriers has shown that the reaction is actually controlled by the Lewis acid/base interaction between the cation and the chloride ion through a concerted mechanism not involving the Bronsted basicity associated with the framework oxygen atoms.

This study highlights the need to make a detailed analysis of reactions catalyzed by basic zeolites because one can easily be misled to think in terms of simple concepts. In this case, LiT_5 proves to be the strongest reactant, in contrast with its expected lower basicity.

The fact that these reactions over basic zeolites go through concerted mechanisms simultaneously involving an acid/base pair in the catalyst is not surprising because a similar situation exists for reactions catalyzed by acid zeolites, where the activity of the Brönsted site is actually dependent on the existence of associated basic sites.

Acknowledgment. C.J.A.M. thanks the CNPq and FINEP/CTPETRO for support. A.R.-S. and C.Z.-W. thank the FOMES2000-SEP for unlimited time on the IBMp690 32-processor supercomputer at UAEM and for support from CONACYT project 34673.

References and Notes

(1) (a) Hathaway, P.; Davis, M. *J. Catal.* **1989**, *116*, 263. (b) D. Barthomeuf, *J. Phys. Chem.* **1984**, *88*, 42−45. Yagi, F.; Kanura, N.; Tsuji, H.; Kita, H.; Hattori, H. *Stud. Surf. Sci. Catal.* **1994**, *90*, 349. (c) Davis, M.; Kim, J.; Li, H.; Chen, C. *Microporous Mater.* **1994**, *2*, 413.

(2) (a) Barthomeuf, D. *J. Phys. Chem.* **1984**, *88*, 42. (b) Mortier, W. *J. Catal.* **1978**, *55*, 138.

(3) Pearson, R. G. *J. Am. Chem. Soc.* **1963**, *85*, 3533.

(4) (a) Murphy, D.; Massiani, P.; Franck, R. Barthomeuf, D. *J. Phys. Chem.* **1996**, *100*, 6731−6738. (b) Huang, M.;S. Kaliaguine, S. *J. Chem. Soc., Faraday Trans.* **1992**, *88*, 751−758.

(5) Hashimoto, S. *Tetrahedron*, **2000**, *56*, 6957−6963.

(6) Huang, M.; Adnot, A.; Kaliaguine, S. *J. Am. Chem. Soc.* **1992**, *114*, 10005.

(7) (a) Mallmann, A.; Barthomeuf, D. *Stud. Surf. Sci. Catal.* **1986**, *28*, 609. (b) Mallmann, A.; Barthomeuf, D. *Zeolites* **1988**, *8*, 292. (c) Ferrari, A. M.; Neyman, K. M.; Huber, S.; Knözinger, H.; Rösch, N. *Langmuir*, **1998**, *14*, 5559.

(8) (a) Gensse, F.; Anderson, T.; Fripiat, J. *J. Phys. Chem.* **1980**, *84*, 3562. (b) King, S.; Garces, J. *J. Catal.* **1987**, *104*, 59. (c) Liu, J.; Ying, P.; Xin Q.; Li, C. *Zeolites*, **1997**, *19*, 197.

(9) (a) Ciambelli, P.; Corbo, P. *Thermochim. Acta* **1988**, *137*, 51. (b) Zeng, J. *Appl. Catal., A* **1995**, *126*, 141.

(10) Smith, T.; Blower, C. *J. Chem. Soc., Faraday Trans.***1994**, *90*, 931.

(11) Mellot, C. F.; Cheetham, A. K.; Harms, S.; Savitz, S.; Gorte R.; Myers, A. L. *J. Am. Chem. Soc.* **1998**, *120*, 5788.

(12) Choi, S. Y.; Park, Y. S.; Hong, S. B.; Yoon, K. B. *J. Am. Chem. Soc.* **1996**, *118*, 9377.

(13) Ranjit, K. T.; Kevan, L. *J. Phys. Chem. B* **2002**, *106*, 1104.

(14) Sánchez- Sánchez, M.; Blasco T.; Rey, F. *Phys. Chem. Chem. Phys.* **1999**, *1*, 4529.

(15) Joshi, U. D.; Joshi, P. N.; Tamhankar, S. S.; Joshi V. V.; Shiralkar, V. P. *J. Phys. Chem. B* **2001**, *105*, 10637.

(16) Vayssilov G. N.; Rösch, N. *J. Phys. Chem. B* **2001**, *105*, 4277.

(17) Heidler, R.; Janseens, G. O. A.; Mortier W. J.; Schoonheydt, R. A. *J. Phys. Chem.* **1996**, *100*, 19728.

(18) Deka, R. Ch.; Roy R. K.; Hirao, K. *Chem. Phys. Lett.*, **2000**, *332*, 576.

(19) Correa, R. J.; Mota, C. J. A. *Phys. Chem. Chem. Phys.* **2002**, *4*, 4268.

(20) Baerlocher, Ch.; Meier, W. M.; Olson, D. H. *Atlas of Zeolite Framework Types*, 5th ed.; Elsevier: Amsterdam, 2001.

(21) Leininger, T.; Nicklass, A.; Kuchle, W.; Stoll, H.; Dolg, M.; Bergner, A. *Chem. Phys. Lett.* **1996**, *255*, 274.

(22) (a) Chirlian, L. E.; Francl, M. M. *J. Comput. Chem.* **1987**, *8*, 894. (b) Breneman, C. M.; Wiberg, W. B. *J. Comput. Chem.* **1990**, *11*, 361.

(23) Frisch, M. J.; Trucks, G. W.; Schlegel, H. B.; Scuseria, G. E.; Robb, M. A.; Cheeseman, J. R.; Zakrzewski, V. G.; Montgomery, J. A., Jr.; Stratmann, R. E.; Burant, J. C.; Dapprich, S.; Millam, J. M.; Daniels, A. D.; Kudin, K. N.; Strain, M. C.; Farkas, O.; Tomasi, J.; Barone, V.; Cossi, M.; Cammi, R.; Mennucci, B.; Pomelli, C.; Adamo, C.; Clifford, S.; Ochterski, J.; Petersson, G. A.; Ayala, P. Y.; Cui, Q.; Morokuma, K.; Malick, D. K.; Rabuck, A. D.; Raghavachari, K.; Foresman, J. B.; Cioslowski, J.; Ortiz, J. V.; Stefanov, B. B.; Liu, G.; Liashenko, A.; Piskorz, P.; Komaromi, I.; Gomperts, R.; Martin, R. L.; Fox, D. J.; Keith, T.; Al-Laham, M. A.; Peng, C. Y.; Nanayakkara, A.; Gonzalez, C.; Challacombe, M.; Gill, P. M. W.; Johnson, B. G.; Chen, W.; Wong, M. W.; Andres, J. L.; Head-Gordon, M.; Replogle, E. S.; Pople, J. A. *Gaussian 98*, revision A.7; Gaussian, Inc.: Pittsburgh, PA, 1998.

(24) Gutmann, V. *The Donor−Acceptor Approach to Molecular Interactions*; Plenum Press: New York, 1978.

(25) Corrêa, R. J. *Tetrahedron Lett.* **2003**, *44*, 7299.